Enabling Fast Discharge Li-ion Batteries via Electrolyte Formulations for Urban Air Mobility Applications

Anuj Bisht[a*], Marm Dixit[a*], Ruhul Amin[a], Rachid Essehli[a], Ali Abouimrane[a], Chol-Bum M. Kweon[b], Ilias Belharouak[a*]

[a] Electrification and Energy Infrastructures Division, Oak Ridge National Laboratory, Oak Ridge, TN 37830, USA
[b] Army Research Directorate, Combat Capabilities Development Command Army Research Laboratory, Aberdeen Proving Ground, MD, 21005, USA

* Corresponding authors: - Anuj Bisht (bishta@ornl.gov)

- Marm Dixit (dixitmb@ornl.gov)

- Ilias Belharouak (belharouaki@ornl.gov)

Abstract

High-power discharge requirements are critical for lithium-ion batteries (LIBs) used in electric Vertical Takeoff and Landing (eVTOL) vehicles that are increasingly considered in urban mobility. This investigation places a particular emphasis on understanding the impact of electrolytes on discharge processes and rate capability. We aim to compare the discharge behavior of LiBs using a conventional electrolyte (Gen 2: 1.2 M LiPF6 in EC:EMC) and the dual salt LiTFSI-LiBOB-based electrolyte. We carefully examine the profiles of charging and discharging, the behavior during extended cycles, impedance spectroscopy results, and the characteristics of the electrode surface. Our research findings demonstrate the complex relationship between the composition of electrolytes and the specific high-power discharge requirements of electric vertical takeoff and landing (eVTOL) systems. This research highlights the importance of customizing electrolyte compositions to optimize energy storage density while simultaneously enabling higher power extraction to enhance performance in short-range electric aviation.

Keywords: Urban air mobility; Lithium-ion batteries; Fast discharge; Rate capability; eVTOL, Electrolyte formulations

1. Introduction

In today's world, the demand for energy is increasing day by day. Whether it is for our smartphones, cars, or the exciting new world of flying taxis called electric Vertical Takeoff and Landing (eVTOL), we need more energy[1-3]. The batteries powering our daily devices are playing a crucial role in this energy revolution, and lithium-ion batteries are leading the way. However, as we move towards new frontiers in aviation, such as eVTOLs vehicles, we need powerful batteries to make them a reality[4-7]. The power requirements become even more demanding, and the batteries need to provide decent amounts of energy super quickly, especially during the eVTOL take-off and landing[6, 8]. Current batteries struggle to meet these high-energy demands, so the research community needs to come up with new solutions[6, 9].

The materials used in the battery are like building blocks, determining how well it can store and release energy. One crucial aspect involves the selection of the right electrolyte and materials for the battery application[2, 10-19]. The electrolyte serves as the bridge for lithium ions to cross between the anode and cathode, while the choice of lithium salts and solvents significantly influences the battery's performance and stability[17, 20]. By carefully designing these components, the battery can meet the high-power demand of eVTOL vehicles while ensuring safety and durability under extreme conditions.

Lithium-ion batteries are a result of advanced chemistry and engineering[21]. The flow of electrical charge between the positive and negative electrodes is enabled by the mobility of lithium ions, which is fundamental to their function. These ions bridge the gap between the negative electrode (typically made of graphite) and the positive electrode (often constructed with compounds containing lithium, nickel, cobalt, and manganese-based oxides)[13]. However, the battery performance is not solely determined by these electrodes. Standard electrolytes have been made of lithium hexafluorophosphate ($LiPF_6$) dissolved in organic solvents[22-24]. It is worth noting that the choice of lithium salt and the precise solvent composition play a crucial role in shaping the battery electrical power and long-term

performance stability[10, 11, 19, 20, 25]. The hypothesis that the dual salt electrolyte may outperform the traditional Gen-2 electrolyte is motivated by previous research [19], which demonstrated improved fast discharging capabilities with the dual salt (LiTFSI + LiBOB) with or without LiPF6 as compared to LiPF6 alone. Additionally, the dual salt electrolytes are known to form a more robust and stable solid-electrolyte interphase (SEI) layer, which can reduce lithium plating and enhance thermal stability. The present study aims to compare the performance of two types of electrolytes, Gen-2 and dual salt electrolyte (LiTFSI-LiBOB)[19], under the high-power demand scenario in an electric vertical takeoff and landing (eVTOL) vehicle (Figure 1a). We examined their charge-discharge profiles, long-term cycling responses, and electrode surface morphologies to understand the interplay between electrolyte systems and rate capability performance. Our research provides insights into the nuanced behavior of these electrolytes in high-power demand applications.

2. Experimental Section

Two distinct electrolytes were employed in this study: Gen-2 and LiTFSI-LiBOB. Gen-2 electrolyte (1.2 M $LiPF_6$ in EC: EMC) was procured and used without further modification. The dual salt electrolyte of 1.0 M concentration was synthesized by combining 0.6 M LiTFSI (1.72 g) and 0.4 M LiBOB (0.774 g) in a 10 mL solution of EC:EMC (3:7 v/v) within an argon-filled glovebox. The resulting solution underwent overnight stirring in the glovebox. A clear solution was obtained because of the complete dissolving of the salts in the solvents which was used for further testing. The CR2032 coin cells were fabricated using NMC811 as the cathode and graphite as the anode with the resulting electrolyte. The loading of NMC811 was standardized at 10 mg/cm², and an N/P ratio (negative electrode capacity to positive electrode capacity) of ≈1.16 was maintained. Cathode and anode punches of 14 mm and 16 mm and Celgard 2325 separators with diameter of 18 mm were utilized for assembling the coin cells. A constant 100 μL quantity of electrolyte was utilized for all the coin cells. All cell assembly procedures were conducted in an inert atmosphere within the argon-filled glovebox.

Electrochemical testing was carried out on a Biologic SP-300 potentiostat with a high-current booster for carrying out high-rate discharge. All electrochemical testing was conducted inside ESPEC thermal chambers maintained at 30±1°C. Initial formation cycles involved a constant current of C/10 from 3.0 V to 4.2 V for three cycles. Subsequent charging was performed at a 1C rate, following an eVTOL discharge profile. In a second set of experiments, cells were subjected to varying temperatures (20 °C, 10 °C, and 0 °C) under similar electrochemical testing conditions. The electrochemical impedance (EIS) was performed in the frequency range of 1MHz to 1hz using a sinusoidal voltage amplitude of 20 mV at OCV conditions. The EIS spectra were fitted using an equivalent circuit model built in ZView software. All the electrochemical testing were performed using a Biologic potentiostat. The equivalent circuit model was designed based on the determination of distribution of relaxation processes. Post-cycling, coin cells were opened within the glovebox, and electrodes were washed with anhydrous dimethyl carbonate (DMC). All cycled samples were in a discharged state. Surface morphology analysis was conducted using a Scios 2 FIB-SEM instrument.

3. Results and Discussion

Figure 1a shows the schematic representation of predicted discharge rate requirements with the state of charge (SOC) for eVTOL profile. The eVTOL mission profile necessitates a high-rate discharge at high SOC at the beginning of discharge for the lift-off hover and climb steps

Table 1 Details of the eVTOL mission profile

Flight Profile	**Hover**	**Climb**	**Cruise**	**Descent**
	6C	2C	C/3	3C
Duration (min)	2	5	45	5
Expected Drain	33%	17%	25%	25%

of the profile (6C and 2C), and an equivalent high-rate discharge at low SOC at the end of discharge for landing hover and descent (3C). **Figure 1b** represents an electric Vertical Take-Off and Landing (eVTOL) flying profile, with a corresponding discharge polarization profile

highlighting the different discharge rates employed within the different segments of the eVTOL flight. It should also be noted that the duration of these individual segments is different and detailed breakdown of the mission profile and expected capacity from each segment is outlined

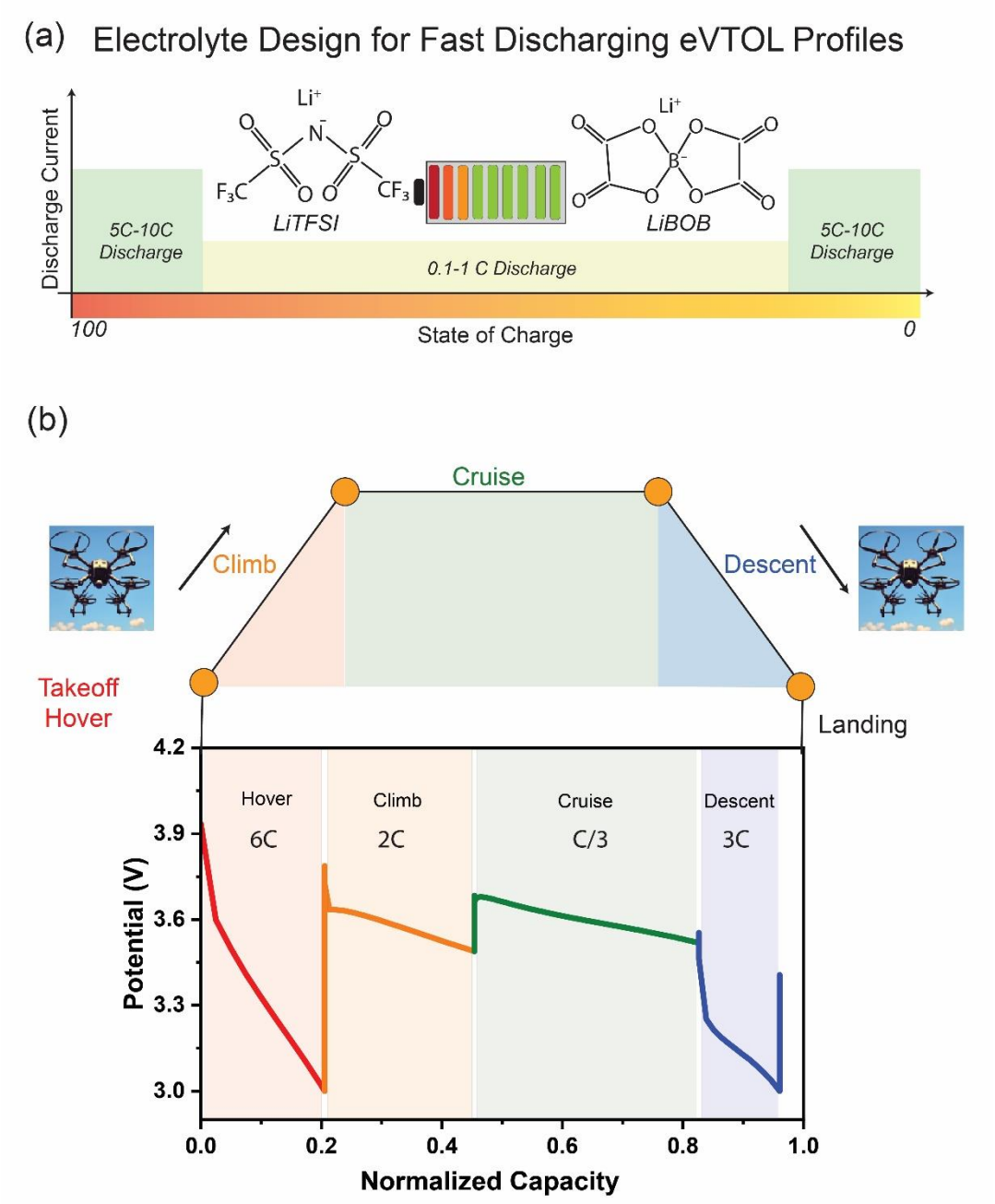

Figure 1. Schematic representation of a) discharge current versus state of charge, illustrating the dual salt electrolyte molecule (LiTFSI-LIBOB) and b) electric Vertical Take-Off and Landing (eVTOL) flying profile, alongside the corresponding discharge current profile during the process.

in **Table 1**. It is seen that the significant polarization voltage drops for the initial hover step, as well as the descent step, while lower polarizations are seen for the climb and the cruise step in general (**Fig. 1b**).

The voltage polarization curve and discharge capacity analysis of cells employing Gen-2 and dual salt electrolyte systems under the Electric Vertical Takeoff and Landing (EVTOL) profile reveal notable distinctions in performance and cycling durability (**Figure 2**). The Gen-2 system exhibits substantial polarization, evident by consistent voltage fade reaching 3 volts even before completing the final descent segment after 100 cycles (**Figure 2a**). This pronounced polarization persists throughout all discharge segments, suggesting a notable decline in performance over repeated cycling. The voltage decay and capacity loss continue with further

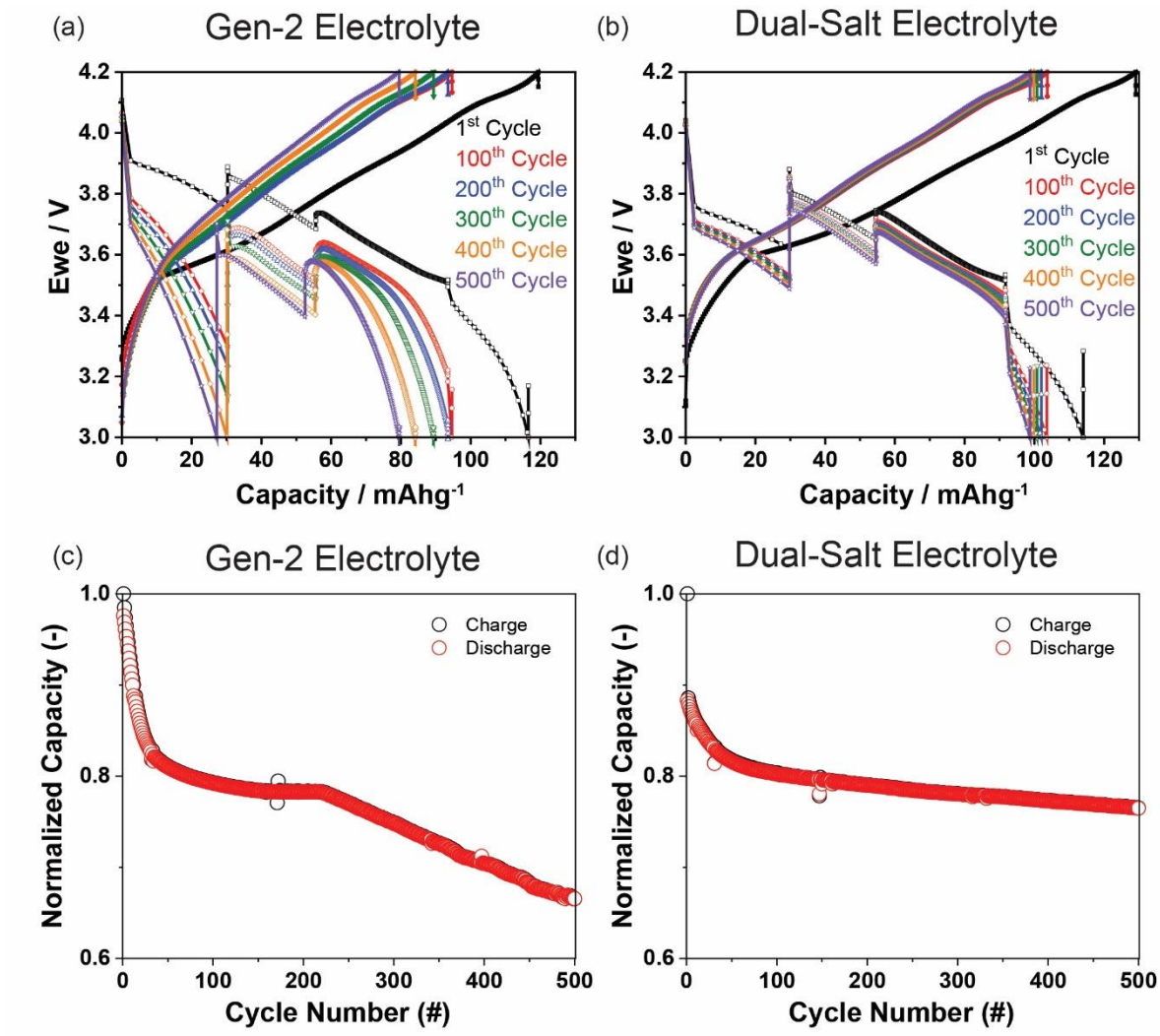

Figure 2. Charging-discharging behavior and capacity fade comparison of coin cell with Gen-2 (a, c) and Dual-salt (b, d) electrolytes over 500 cycles.

cycling leading to rapid deterioration in performance. Notably, the absence of the descent discharge segment within first 100 cycles indicates the inadequacy of Gen-2 electrolyte to provide energy or power to mission essential segments. In contrast, the dual-salt electrolyte system shows stable cycling performance over 500 cycles with limited voltage decay as well as capacity fade. All discharge segments are achieved across 500 cycles which is a significant improvement over <100 cycles observed with the Gen-2 system. These results indicate a significant enhancement in cell performance can be achieved by tailoring the electrolyte chemistry for the demanding load profile of electric Vertical Takeoff and Landing (eVTOL) vehicles. It is anticipated the partial degradation of Gen-2 electrolyte by running the cell in the eVTOL protocol possibly enhanced the total cell resistance.

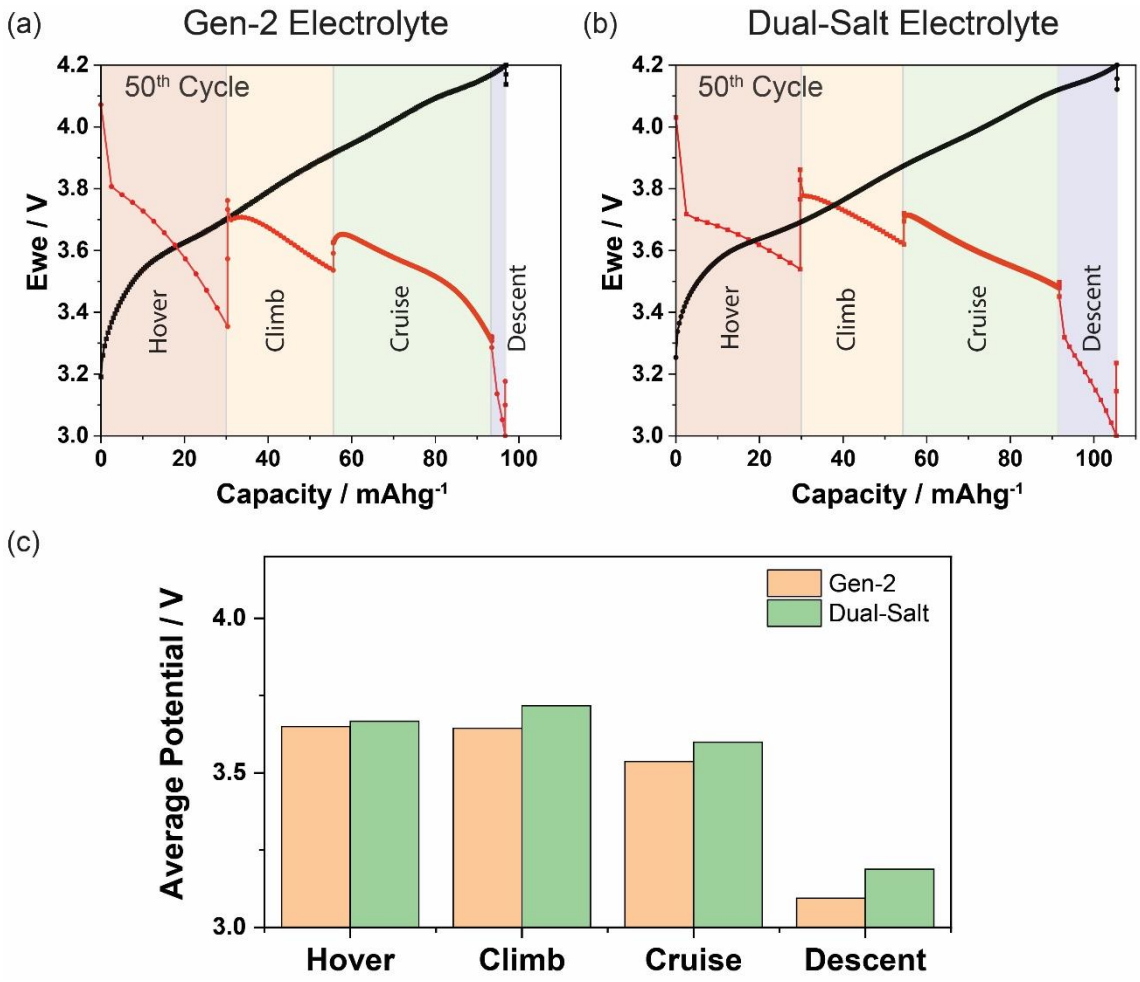

Figure 3. 50th cycle comparison of charge/discharge in a) Gen-2 and b) Dual-Salt electrolytes. c) Bar graph of average potential in each segment for both electrolytes.

A snapshot of the discharge curves for both the systems for the 50th cycle is presented in Figure 3. Both cells with Gen-2 and dual salts show identical charge capacity, however, the discharge profiles are extremely different. The Gen-2 system clearly shows much higher polarization in

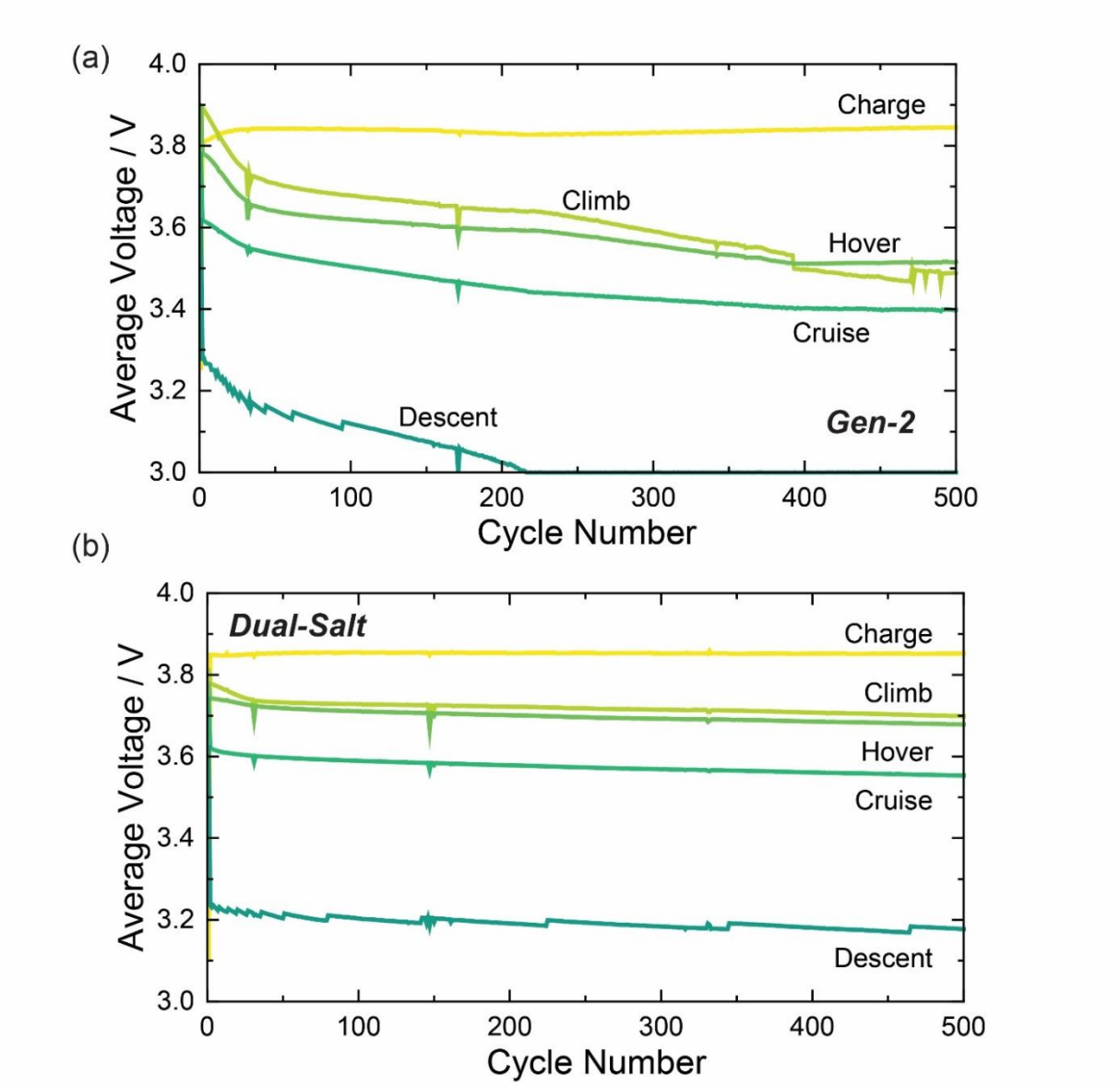

Figure 4. Average voltage in each segment versus cycle number in (a) Gen-2 and (b) Dual-Salt Electrolyte.

all discharge segments compared to the dual-salt electrolyte indicating a resistive behavior or transport limitations within the cell. This difference is clearly illustrated in Figure 3c, which displays a bar chart of the average potential versus each operational segment. It becomes

evident that the dual salt electrolyte consistently maintains higher potential levels in every operational segment compared to the Gen-2 system. For example, for the descent segment the Gen-2 systems shows an average potential of 3.15V compared to 3.2 V observed for the dual-salt system. In general, ~1-2% improvement in the average potential was observed for the 50th cycle in the different segments. For more detailed insight into the long-term performance of these cells, the average potential evaluated over 500 cycles individually is presented in Figure 4 for each segment of the eVTOL profile for the two different electrolyte media.

The evaluation of the average voltage in each segment over the cycle life provides valuable insights into the electrochemical stability of the system. Notably, the descent segment polarization quickly drops while the climb segment shows a consistent fade over the cycling duration. In contrast, the average potential measurements in individual segments of the dual salt electrolyte show very stable behavior. The average polarization data prominently highlights the enhanced stability achieved with the dual-salt electrolyte. This finding highlights the significance of electrolyte composition in influencing the overall electrochemical performance of the eVTOL system. To gain detailed insights into the difference of cell polarization impedance measurements were performed before and after cycling. The impedance spectra show distinct profiles for Gen-2 and dual salt electrolyte as shown in Figure 5. Here we have shown EIS spectra after 1^{st}, 10^{th} and 500^{th} EVTOL cycling protocol for Gen-2 (Figure 5a) and dual salt electrolyte (Figure 5b). The two electrolytes exhibit very different cell resistance at different cycling states. It is discernible from the Figure 5 that after the 1st eVTOL cycle the total cell resistance decreases and again increases for Gen-2 electrolyte (Figure 5a) while dual salt electrolyte (Figure 5b) displays a gradual decrease of total cell resistance and remains constant on further cycling. To understand the insight into the change of cell resistance with cycling of two electrolytes, we calculated distributions of relaxation times after formation cycle and after 500 cycles. The cells with two electrolytes exhibit two different distributions of relaxation processes after 500 cycles (supplementary **Figure S2 and S3**). In the formation cycle,

both the electrolyte systems display five relaxation processes while after 500 cycles dual salt electrolyte exhibits additional processes. Based on the relaxation process equivalent circuits were designed (supplementary **Figure S2 and S3**) and individual resistances were separated for after formation cycle and after 500 cycles and are compared in Table S1.

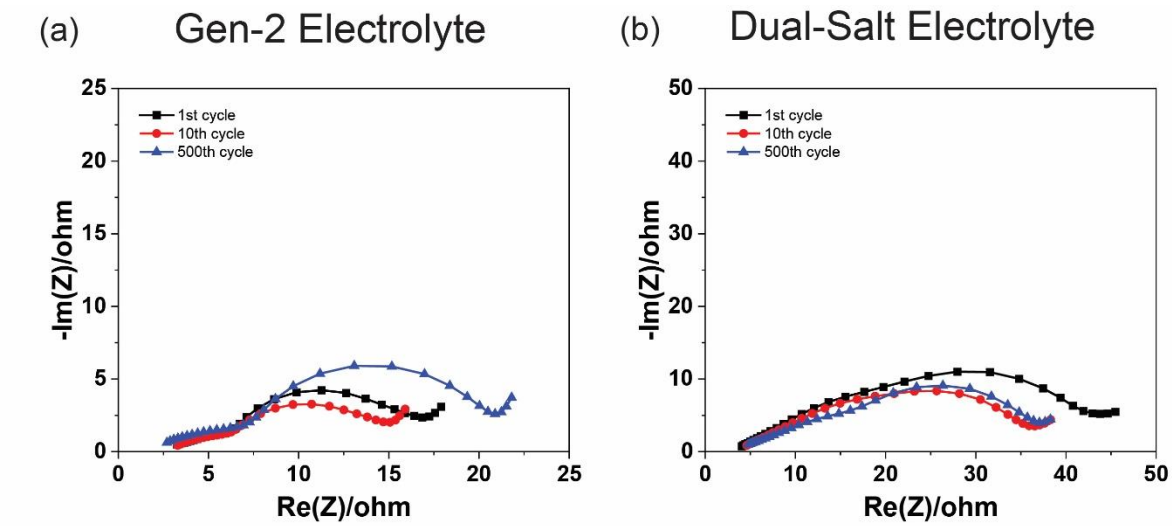

Figure 5. Electrochemical impedance spectroscopy (EIS) spectra after 1, 10, and 500 cycles (a) Gen-2 electrolyte and (b) Dual-Salt electrolyte.

It is interesting to notice that the Ohmic resistance of electrolyte solution does not change between the formation and 500th cycles, whereas the lower frequency interface resistance changes significantly (Cf. table S1). The lower frequency interfacial resistance after formation to 500 cycles changes from 73Ω to 15Ω for the dual salt electrolyte. It should also be noted that huge changes of interfacial resistance between formation cycle and first eVTOL cycle was observed for dual salt electrolyte and insignificant change was observed for Gen-2 electrolyte. Both these results indicate that the presence of a beneficial SEI layer on the anode with the dual-salt electrolyte that is formed after the eVTOL cycling protocol that facilitates lithium-ion transport and stabilizes the anode. On the contrary, the lower frequency resistance of cell with Gen-2 electrolyte increases from 7Ω to 13Ω between formation and 500th cycles. This is indicative of formation of resistive layers and could also arise from presence of dead Li on the

anode surface. It should be noted that other resistive processes almost remain constant (Cf. Table S1). The differences observed between the two electrolytes can be attributed to their distinct electrochemical properties and stability. The initial high resistance in both cases is typical for the first cycle due to various initial processes at the electrode-electrolyte interface. The reduction in impedance after 10 cycles in the Dual Salt electrolyte suggests favorable long-term stability, while the increase in impedance in GEN-2 after 500 cycles highlights its limitations. The obtained cell resistances for Gen-2 and dual salts are very much consistent with the discharge voltage profile observed in the eVTOL protocol.

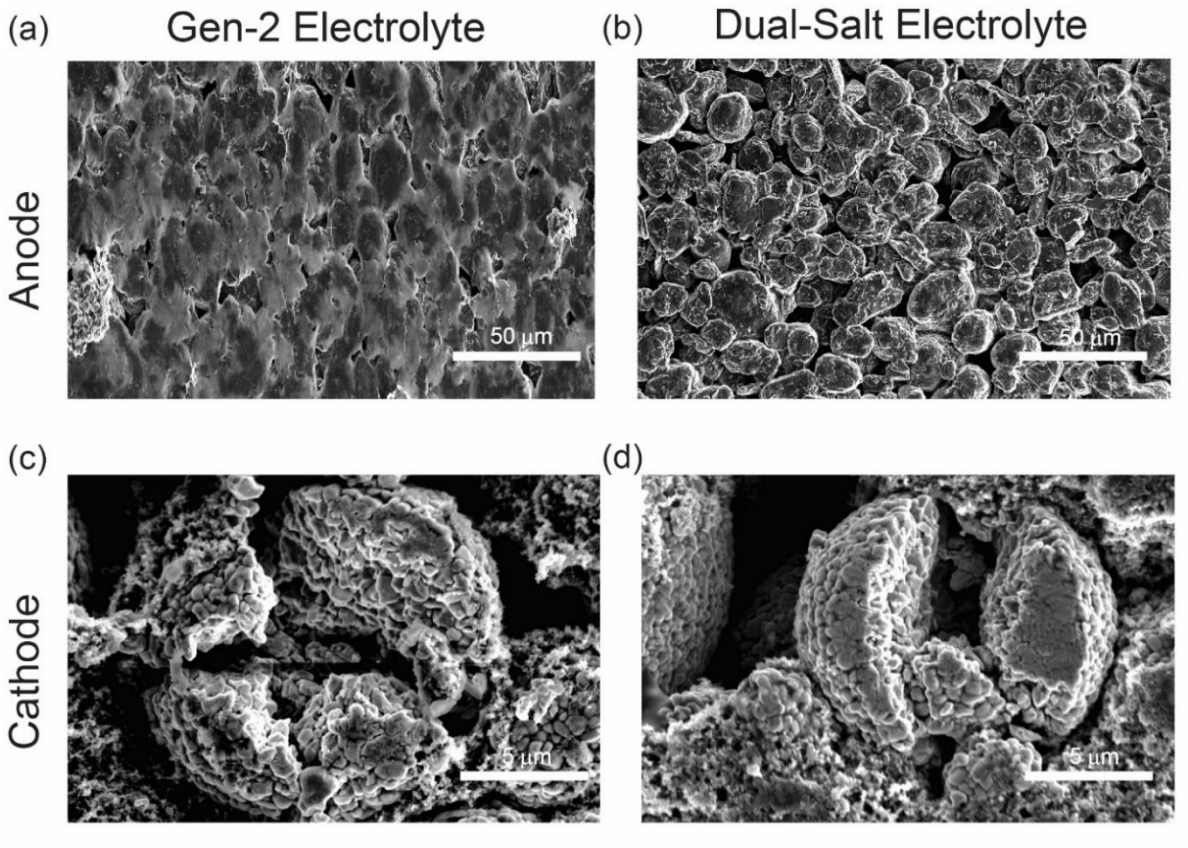

Figure 6. SEM Images of 500-Cycled Cells in Gen-2 and Dual-Salt Electrolytes. (a) Anode and (c) Cathode for Gen-2 Electrolyte. (b) Anode and (d) Cathode for Dual-Salt Electrolyte.

After the cycling tests, we disassembled the coin cells and conducted a thorough examination of the surface morphologies of the washed electrodes (Figure 6). Figures 6a and 6b present scanning electron microscopy (SEM) images of the cycled anode for Gen-2 and dual salt electrolyte systems respectively. **In Figure 6a**, it is quite evident that the anode cycled with

Gen-2 electrolyte exhibits clear indications of lithium plating. In contrast, **Figure 6b**, which represents the anode cycled with the dual salt electrolyte, does not show any signs of lithium plating. When we examine the SEM images of the cycled cathodes in **Figure 6c** and **6d**, we observe that both systems display spherical particles with evidence of particle cracking in both the Gen-2 and dual salt electrolyte systems. This microscopic analysis provides visual confirmation of the differences in electrode behavior between the two electrolyte systems, particularly highlighting the absence of lithium plating in the dual salt electrolyte system, which contributes to its enhanced performance in the eVTOL application.

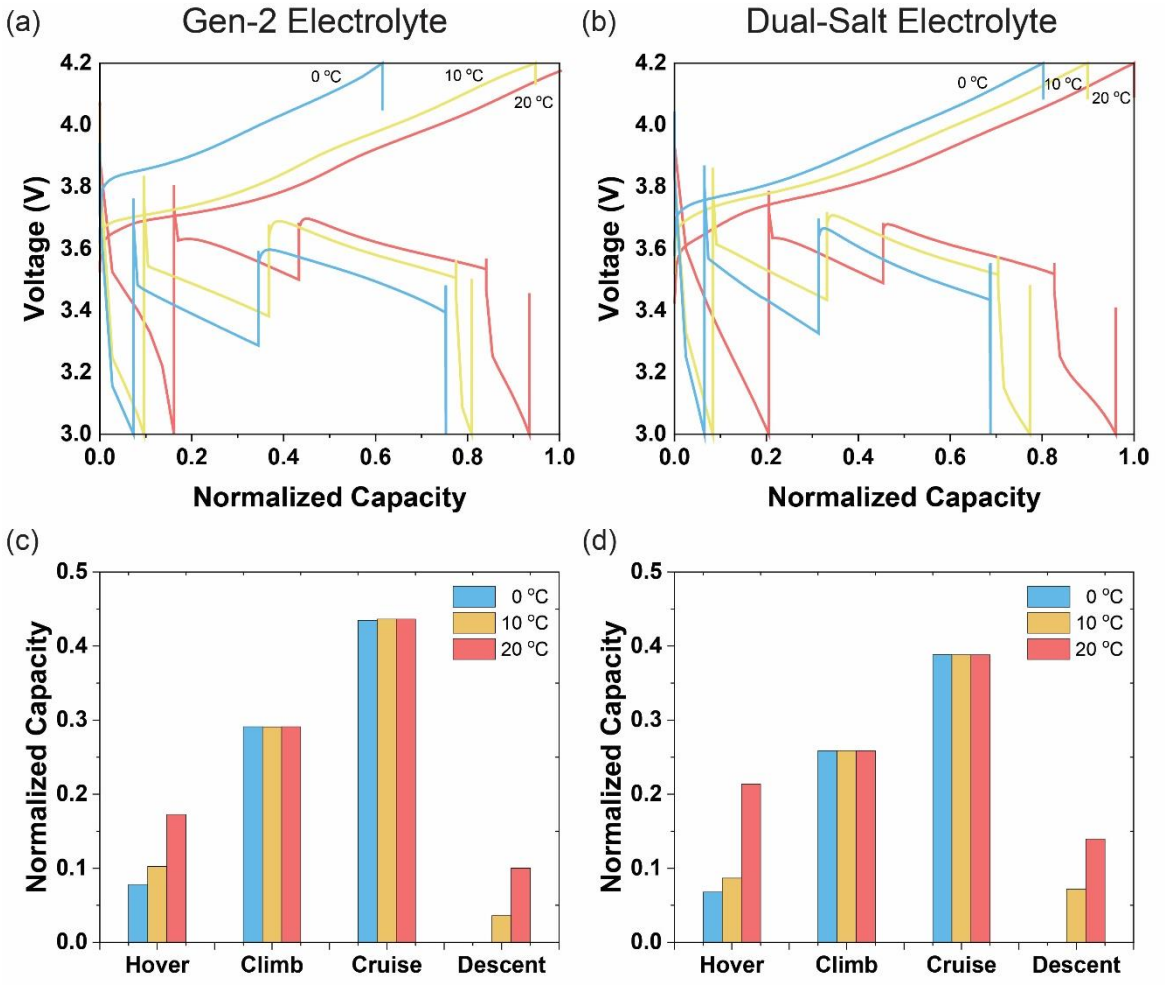

Figure 7. The charging and discharging behavior at 20°C, 10°C, and 0°C in a) Gen-2 and b) Dual-Salt Electrolytes. Bar graphs of normalized capacity in each segment at 20°C, 10°C, and 0°C in c) Gen-2 and d) dual-salt electrolyte.

Temperature tolerance is a key metric for eVTOL energy storage systems as they are subjected to lower temperatures at higher altitudes as well as from different geographical locations. To

gain deeper insights into the temperature impact on the eVTOL profile discharge, Gen-2 and dual salt electrolyte coin cells were subjected to testing at three different temperatures: 0°C, 10°C, and 20°C, as shown in **Figure 7**. The charge and discharge profiles of both systems closely resemble each other. We have also included data on the normalized capacity for each segment at these varying temperatures (**Fig. 7c, d**). It's worth noting that at 0°C, neither system demonstrated any capacity in the descent region. When comparing the performance in the hover and descent regimes, it becomes evident that at 20°C, the dual salt electrolyte outperformed Gen-2 by exhibiting a higher capacity, suggesting a greater power output in the former. However, at lower temperatures, the dual-salt shows equivalent or even poor performance compared to the Gen-2 electrolyte. **Figure S1** illustrates the conductivity of both the dual-salt and gen-2 electrolyte systems at different temperatures (30°C, 20°C, 10°C, and 0°C). Surprisingly, we see that the dual-salt electrolyte system shows lower conductivity throughout the temperature range investigated. This can help explaining the cycling behavior observed at different temperatures. At lower temperatures, a notable decline in performance was observed. The larger salts in the dual-salt formulation hinder the mobility of the electrolyte, resulting in detrimental performance. In contrast, at room temperature, the potentially higher transference numbers contribute to mitigating and even enhancing the high-rate performance, despite the lower overall conductivity. Also, it indicates the lower polarizability of the dual salt electrolyte compared to Gen-2. These temperature-dependent behaviors highlight the nuanced performance characteristics of the dual-salt and gen-2 electrolyte systems, offering valuable insights for their application in diverse environmental conditions.

4. Conclusion

In this work, we compared the performance of two electrolyte systems, Gen-2 and the dual salt electrolyte, in the demanding context of electric Vertical Takeoff and Landing (eVTOL) applications. Our investigation involved a detailed examination of charge-discharge profiles, long-term cycling responses, electrode surface morphologies and analysis of individual

resistive components before and after long eVTOL cycling. Throughout 500 cycles, the Gen-2 system exhibited signs of polarization and capacity loss, especially noticeable during high-rate hover and descent phases. In contrast, the dual salt electrolyte system displayed remarkable stability, retaining both capacity and maintaining low polarization potentials drop throughout the cycling. Furthermore, when examining the electrode surface morphologies, we observed a noteworthy absence of lithium plating in the dual salt electrolyte system. In summary, our comprehensive evaluation demonstrates that the dual salt electrolyte system outperforms the Gen-2 electrolyte in the context of eVTOL load profiles. Its superior stability, capacity retention, and lower polarization potentials make it a promising candidate for advanced energy storage solutions in electric aviation. This research contributes valuable insights to the ongoing efforts to enhance the reliability and efficiency of energy storage systems in the rapidly evolving field of eVTOL technology.

Supporting Information

Supporting Information is available.

Acknowledgements

This research at Oak Ridge National Laboratory, managed by UT Battelle, LLC, for the US Department of Energy under contract DE-AC05- 00OR22725, was sponsored by the US Army DEVCOM Army Research Laboratory and was accomplished under Support Agreement 2371-Z469-22. The views and conclusions contained in this document are those of the authors and should not be interpreted as representing the official policies, either expressed or implied, of the DEVCOM Army Research Laboratory or the U.S. Government.

References

[1] J. Deng, C. Bae, A. Denlinger, T. Miller, Electric Vehicles Batteries: Requirements and Challenges, Joule, 4 (2020) 511-515.

[2] J.B. Goodenough, K.-S. Park, The Li-Ion Rechargeable Battery: A Perspective, Journal of the American Chemical Society, 135 (2013) 1167-1176.

[3] A. Manthiram, An Outlook on Lithium Ion Battery Technology, ACS Central Science, 3 (2017) 1063-1069.

[4] A. Kasliwal, N.J. Furbush, J.H. Gawron, J.R. McBride, T.J. Wallington, R.D. De Kleine, H.C. Kim, G.A. Keoleian, Role of flying cars in sustainable mobility, Nat Commun, 10 (2019) 1555.

[5] S. Sripad, V. Viswanathan, The promise of energy-efficient battery-powered urban aircraft, Proceedings of the National Academy of Sciences, 118 (2021) e2111164118.

[6] X.-G. Yang, T. Liu, S. Ge, E. Rountree, C.-Y. Wang, Challenges and key requirements of batteries for electric vertical takeoff and landing aircraft, Joule, 5 (2021) 1644-1659.

[7] M. Mitici, B. Hennink, M. Pavel, J. Dong, Prognostics for Lithium-ion batteries for electric Vertical Take-off and Landing aircraft using data-driven machine learning, Energy and AI, 12 (2023) 100233.

[8] A. Ayyaswamy, B.S. Vishnugopi, P.P. Mukherjee, Revealing hidden predicaments to lithium-ion battery dynamics for electric vertical take-off and landing aircraft, Joule, 7 (2023) 2016-2034.

[9] M. Dixit, Balancing battery safety and performance for electric vertical takeoff and landing aircrafts, Device, 1 (2023) 100172.

[10] Z. Du, D.L. Wood, I. Belharouak, Enabling fast charging of high energy density Li-ion cells with high lithium ion transport electrolytes, Electrochemistry Communications, 103 (2019) 109-113.

[11] Z. Du, Z. Yang, R. Tao, V. Shipitsyn, X. Wu, D.C. Robertson, K.M. Livingston, S. Hagler, J. Kwon, L. Ma, I.D. Bloom, B.J. Ingram, A Novel High-Performance Electrolyte for Extreme Fast Charging in Pilot Scale Lithium-Ion Pouch Cells, Batteries & Supercaps, 6 (2023) e202300292.

[12] M. Li, M. Feng, D. Luo, Z. Chen, Fast Charging Li-Ion Batteries for a New Era of Electric Vehicles, Cell Reports Physical Science, 1 (2020) 100212.

[13] Y. Liu, Y. Zhu, Y. Cui, Challenges and opportunities towards fast-charging battery materials, Nature Energy, 4 (2019) 540-550.

[14] E.R. Logan, J.R. Dahn, Electrolyte Design for Fast-Charging Li-Ion Batteries, Trends in Chemistry, 2 (2020) 354-366.

[15] Y. Wang, W.-H. Zhong, Development of Electrolytes towards Achieving Safe and High-Performance Energy-Storage Devices: A Review, ChemElectroChem, 2 (2015) 22-36.

[16] D.L. Wood, J. Li, S.J. An, Formation Challenges of Lithium-Ion Battery Manufacturing, Joule, 3 (2019) 2884-2888.

[17] K. Xu, Electrolytes and Interphases in Li-Ion Batteries and Beyond, Chemical Reviews, 114 (2014) 11503-11618.

[18] J. Zhao, C. Song, G. Li, Fast-Charging Strategies for Lithium-Ion Batteries: Advances and Perspectives, ChemPlusChem, 87 (2022) e202200155.

[19] J. Zheng, M.H. Engelhard, D. Mei, S. Jiao, B.J. Polzin, J.-G. Zhang, W. Xu, Electrolyte additive enabled fast charging and stable cycling lithium metal batteries, Nature Energy, 2 (2017) 17012.

[20] Y.S. Meng, V. Srinivasan, K. Xu, Designing better electrolytes, Science, 378 eabq3750.

[21] T. Horiba, T. Maeshima, T. Matsumura, M. Koseki, J. Arai, Y. Muranaka, Applications of high power density lithium ion batteries, Journal of Power Sources, 146 (2005) 107-110.

[22] W.B. Hawley, A. Parejiya, Y. Bai, H.M. Meyer, D.L. Wood, J. Li, Lithium and transition metal dissolution due to aqueous processing in lithium-ion battery cathode active materials, Journal of Power Sources, 466 (2020) 228315.

[23] A. Kukay, R. Sahore, A. Parejiya, W. Blake Hawley, J. Li, D.L. Wood, Aqueous Ni-rich-cathode dispersions processed with phosphoric acid for lithium-ion batteries with ultra-thick electrodes, Journal of Colloid and Interface Science, 581 (2021) 635-643.

[24] D. Parikh, T. Christensen, J. Li, Correlating the influence of porosity, tortuosity, and mass loading on the energy density of LiNi0.6Mn0.2Co0.2O2 cathodes under extreme fast charging (XFC) conditions, Journal of Power Sources, 474 (2020) 228601.

[25] X. Wu, L. Ma, J. Liu, K. Zhao, D.L. Wood, Z. Du, Understanding the effect of salt concentrations on fast charging performance of Li-ion cells, Journal of Power Sources, 545 (2022) 231863.